Fig. S1.

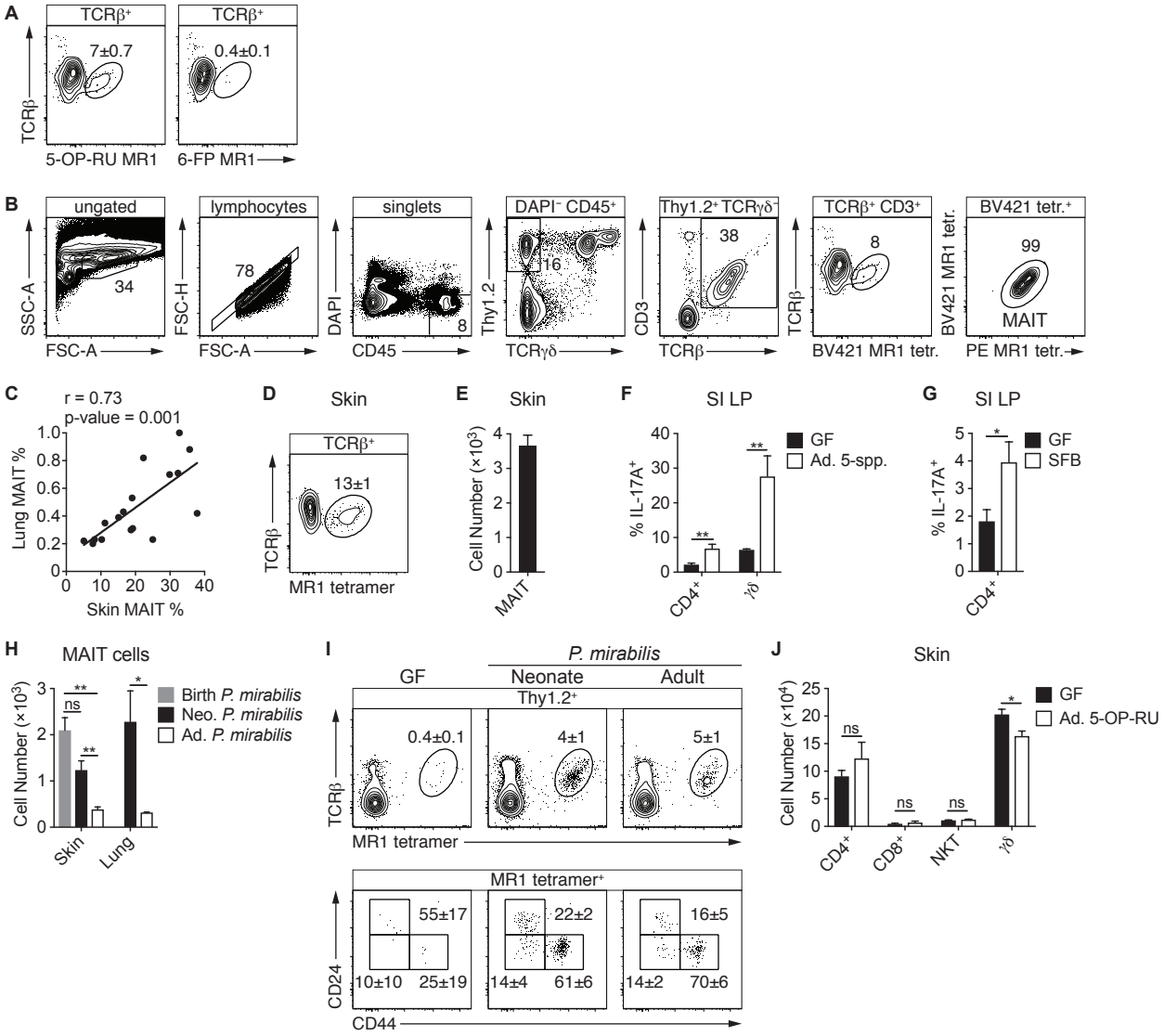

Early-life exposure to riboflavin-synthesizing commensals is required for MAIT cell development. (**A**) Flow cytometry of TCRβ^+ lymphocytes within the skin of SPF mice stained with MR1 tetramer loaded with either 5-OP-RU or 6-FP as a negative control. (**B**) Flow cytometry plots depicting the gating scheme for MAIT cells in the skin. (**C**) Percentage of MAIT cells among $\alpha\beta$ T cells within the indicated organs of SPF WT mice, with each dot representing an individual animal. Pearson's correlation coefficient (r) and p-value of the correlation are denoted. (**D-E**) (**D**) Flow cytometry of TCRβ^+ lymphocytes within the skin of SPF mice and (**E**) the number of cutaneous MAIT cells. (**F**) Frequency of IL-17A$^+$ cells among CD4$^+$ and $\gamma\delta$ T cells from the small intestine (SI) lamina propria (LP) of GF controls and GF mice colonized with the 5-species (5-spp.) community as adults (Ad.). (**G**) Frequency of IL-17A$^+$ cells among CD4$^+$ T cells from the SI LP of

GF controls and GF mice colonized with SFB as neonates. (**H**) Number of MAIT cells in the ear skin and lung tissue of GF mice administered oral gavages of *Proteus mirabilis* either as neonates (Neo.) or adults (Ad.) or exposed to *P. mirabilis* from birth to mothers that were gavaged. (**I**) Flow cytometry of MR1 tetramer-enriched thymocytes from GF controls and GF mice administered oral gavages of *P. mirabilis* either as neonates or adults. (**J**) Number of T cells in the skin of GF controls and GF mice that received weekly topical applications of 5-OP-RU as 7-week-old adults (Ad.). Flow cytometry gate frequencies and graphs indicate means ± SEM. Data represent at least two experiments with four or more mice per group. *$p<0.05$ and **$p<0.01$ as calculated by Student's *t*-test. "ns" denotes that comparison was not significant.

Fig. S2.

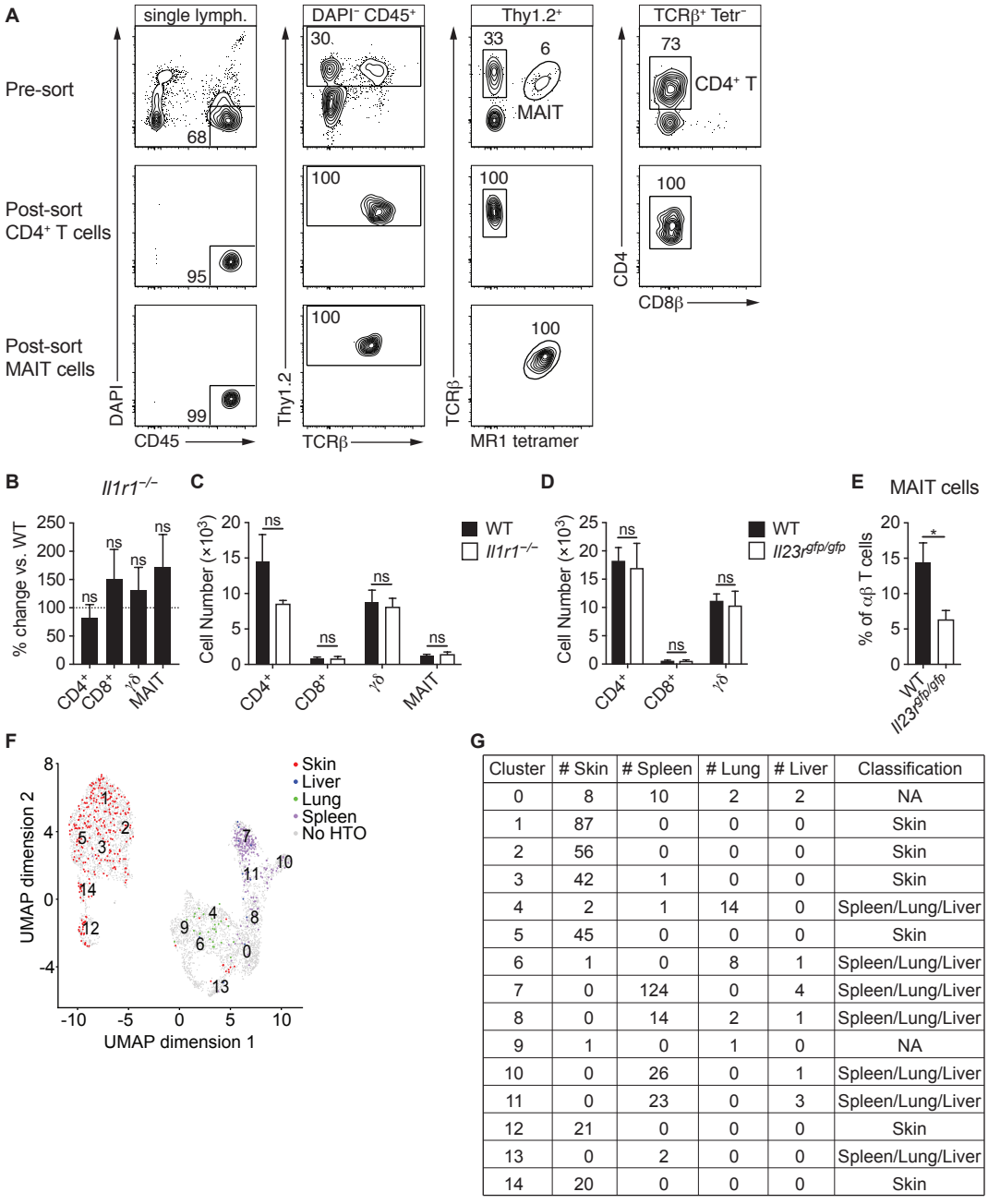

Cluster	# Skin	# Spleen	# Lung	# Liver	Classification
0	8	10	2	2	NA
1	87	0	0	0	Skin
2	56	0	0	0	Skin
3	42	1	0	0	Skin
4	2	1	14	0	Spleen/Lung/Liver
5	45	0	0	0	Skin
6	1	0	8	1	Spleen/Lung/Liver
7	0	124	0	4	Spleen/Lung/Liver
8	0	14	2	1	Spleen/Lung/Liver
9	1	0	1	0	NA
10	0	26	0	1	Spleen/Lung/Liver
11	0	23	0	3	Spleen/Lung/Liver
12	21	0	0	0	Skin
13	0	2	0	0	Spleen/Lung/Liver
14	20	0	0	0	Skin

Cutaneous MAIT cells express a type-17 transcriptional program and require homeostatic IL-23. (**A**) Flow cytometry plots depicting how MAIT and CD4$^+$ T cells were sorted as well as post-sort purity for the RNA-sequencing (RNA-seq) in Fig. 2C-D. Lymphocytes is abbreviated “lymph.” (**B**) Percentage change of the indicated T cells in the skin of *Il1r1*$^{-/-}$ mice compared to WT controls. Statistics denote whether the percentage differs significantly from the WT mean (100%). (**C**) Number of T cells in the skin of *Il1r1*$^{-/-}$ mice and WT controls. (**D-E**) (**D**) Number of T cells and (**E**)

frequency of MAIT cells in the skin of *Il23r*$^{gfp/gfp}$ mice and WT controls. (**F-G**) Single-cell RNA-seq (scRNA-seq) data of MAIT cells sorted from murine skin, spleen, lung, and liver. (**F**) UMAP plot displaying the distribution of clusters and the hashtag oligonucleotides (HTOs) used to distinguish tissues. (**G**) Table displaying the number of HTOs within each cluster. Clusters were assigned to "Skin" or "Spleen/Lung/Liver" based on the presence of HTOs from those tissues. Clusters that did not have a predominance of HTOs from either skin or the other tissues were not assigned ("NA")**.** Flow cytometry gate frequencies and graphs indicate means ± SEM. Data represent at least two experiments with four or more mice per group. **p*<0.05 as calculated by Student's *t*-test. "ns" denotes that comparison was not significant.

Fig. S3.

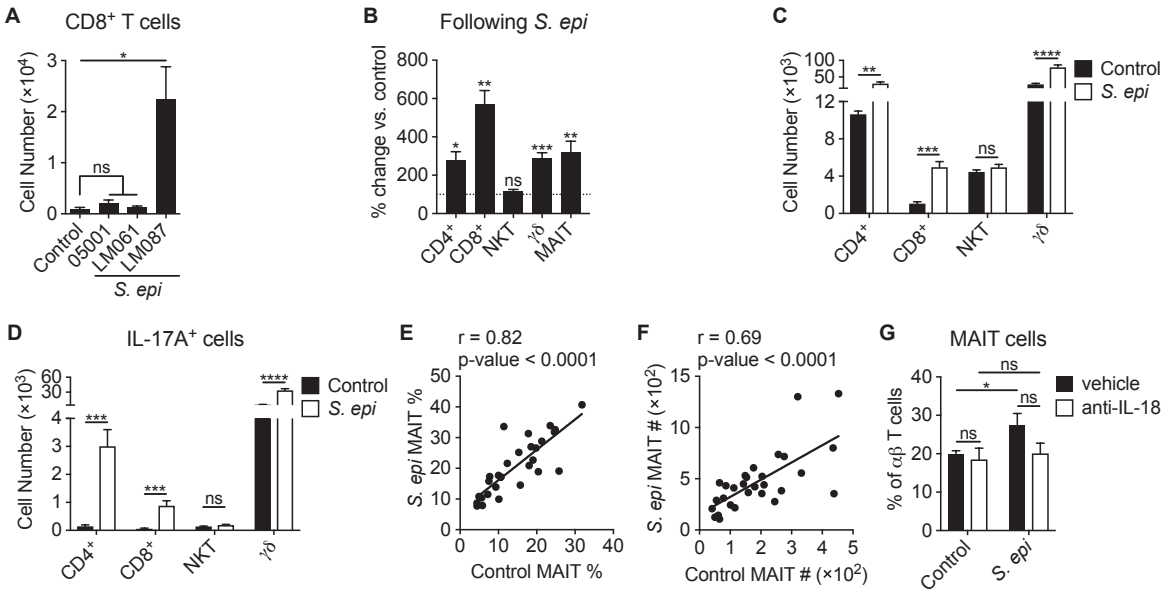

Skin-resident MAIT cells respond to cutaneous microbes in an IL-1- and IL-18-dependent manner. (**A**) Number of cutaneous CD8$^+$ T cells following topical association with the indicated strains of *S. epidermidis* compared to unassociated (control) mice. (**B-D**) (**B**) Percentage change of the indicated T cells in the skin of mice associated with *S. epidermidis* LM061 compared to unassociated controls. Statistics denote whether the percentage differs significantly from the control mean (100%). (**C**) Number of T cells and (**D**) IL-17A$^+$ T cells in the skin of *S. epidermidis*-associated mice and controls. (**E-F**) The initial frequency of MAIT cells in WT mice was determined by analyzing a 4 mm punch biopsy of the left ear. 1 week later, the right ear was associated with *S. epidermidis* LM061 and a 4 mm punch biopsy of the right ear was taken 14 days after the initial association. The MAIT cell (**E**) percentage of αβ T cells and (**F**) number within the 4 mm punch biopsies are displayed for each animal before (control) and after *S. epidermidis* association (*S. epi*) on the *x*-axis and *y*-axis, respectively. Pearson's correlation coefficient (r) and *p*-value of the correlation are denoted. (**G**) WT mice were injected intraperitoneally with either 1 mg of anti-IL-18 antibody or saline (vehicle) 2 days before the initial application of *S. epidermidis* LM061 on day 0 and again on days 1, 5, 8, and 11. The frequency of cutaneous MAIT cells among αβ T cells is displayed. Graphs indicate means ± SEM. Data represent at least two experiments with four or more mice per group. **p*<0.05, ***p*<0.01, ****p*<0.001, and *****p*<0.0001 as calculated by Student's *t*-test. "ns" denotes that comparison was not significant.

Fig. S4.

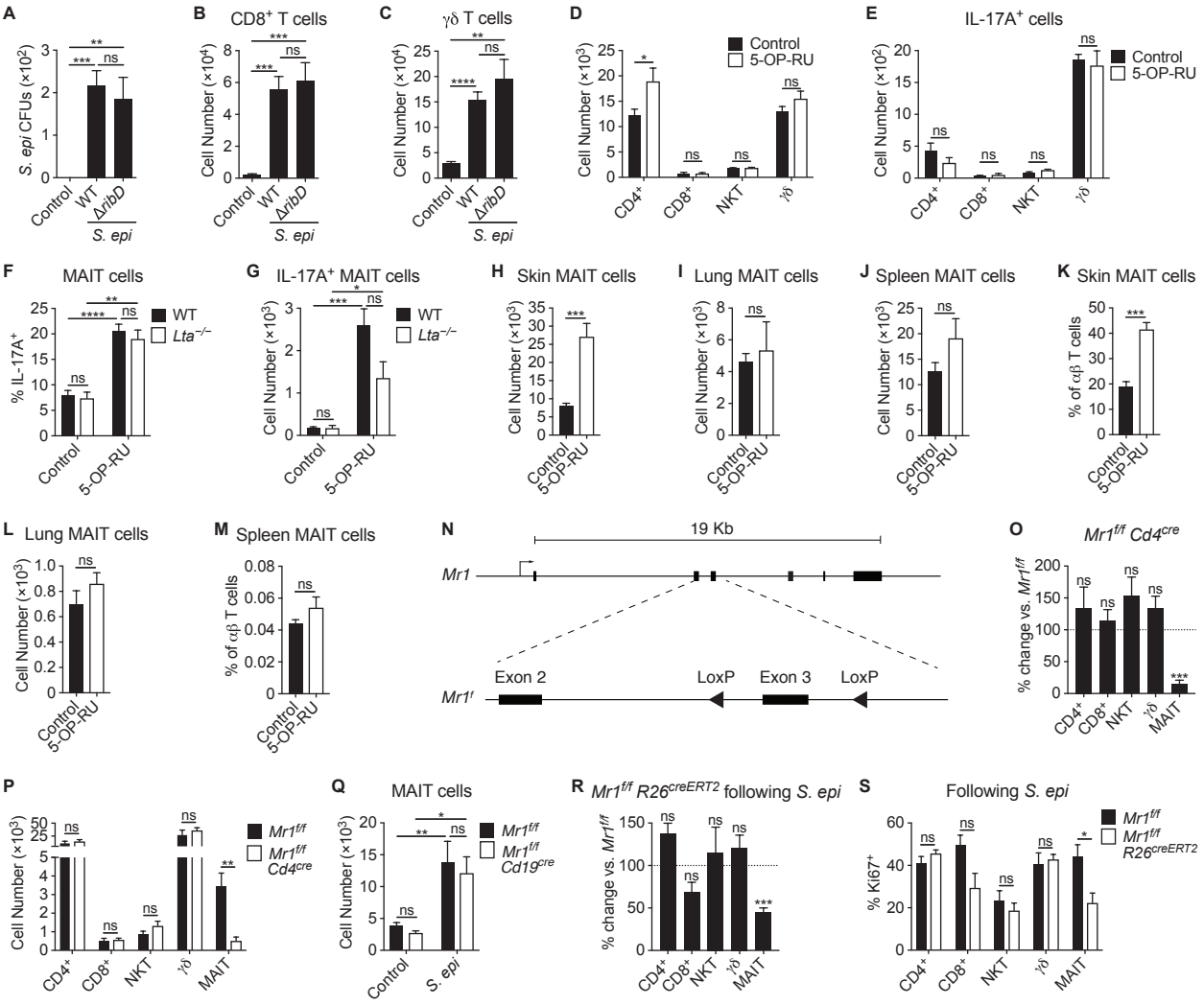

MR1-mediated presentation of riboflavin metabolites is necessary and sufficient for MAIT cell recognition of skin commensals. (**A-C**) WT mice were associated with either *S. epidermidis* LM087 or mutant *S. epidermidis* LM087 Δ*ribD* on days 0, 2, 4, and 6, and analyzed 14 days after the initial application. (**A**) Colony-forming units (CFUs) of *S. epidermidis* after swabbing the ears of associated mice. Number of (**B**) CD8$^+$ and (**C**) γδ T cells following association with either *S. epidermidis* LM087 or mutant *S. epidermidis* LM087 Δ*ribD*. (**D-E**) 5-OP-RU was topically applied to the skin of WT mice on days 0, 2, 4, and 6. 14 days after the initial application, animals were compared to untreated (control) mice. Number of (**D**) T cells and (**E**) IL-17A$^+$ T cells. (**F-G**) Number of cutaneous (**F**) MAIT and (**G**) IL-17A$^+$ MAIT cells from *Lta*$^{-/-}$ and WT mice topically treated with 5-OP-RU and untreated controls. (**H-M**) The (**H-J**) number and (**K-M**) frequency of MAIT cells in the indicated tissues of WT mice topically treated with 5-OP-RU and untreated controls. (**N**)

Diagram depicts the position of LoxP sites flanking the third exon in the floxed-*Mr1* (*Mr1*^{f}) allele. (**O**) Percentage change of the indicated T cells in the skin of *Mr1*$^{f/f}$ *Cd4*^{cre} mice compared to *Mr1*$^{f/f}$ littermate controls. Statistics denote whether the percentage differs significantly from the *Mr1*$^{f/f}$ mean (100%). (**P**) Number of T cells in the skin of *Mr1*$^{f/f}$ *Cd4*^{cre} mice and *Mr1*$^{f/f}$ littermate controls. (**Q**) Number of cutaneous MAIT cells in *Mr1*$^{f/f}$ *Cd19*^{cre} mice and *Mr1*$^{f/f}$ littermates that were associated with *S. epidermidis* LM061 or left as untreated controls. (**R-S**) *Mr1*$^{f/f}$ *R26*^{creERT2} mice and *Mr1*$^{f/f}$ littermates were injected intraperitoneally with 3 mg of tamoxifen 8, 6, 4, and 2 days prior to the initial association with *S. epidermidis* LM061 and were analyzed 14 days later. (**R**) Percentage change of the indicated T cells in the skin of *Mr1*$^{f/f}$ *R26*^{creERT2} mice compared to *Mr1*$^{f/f}$ littermates. Statistics denote whether the percentage differs significantly from the *Mr1*$^{f/f}$ mean (100%). (**P**) Percentage of Ki67^{+} cells among the indicated T cell populations from in the skin of *Mr1*$^{f/f}$ *R26*^{creERT2} mice and *Mr1*$^{f/f}$ littermates. Graphs indicate means ± SEM. Data represent at least two experiments with four or more mice per group. *p<0.05, **p<0.01, ***p<0.001, and ****p<0.0001 as calculated by Student's t-test. "ns" denotes that comparison was not significant.

Fig. S5.

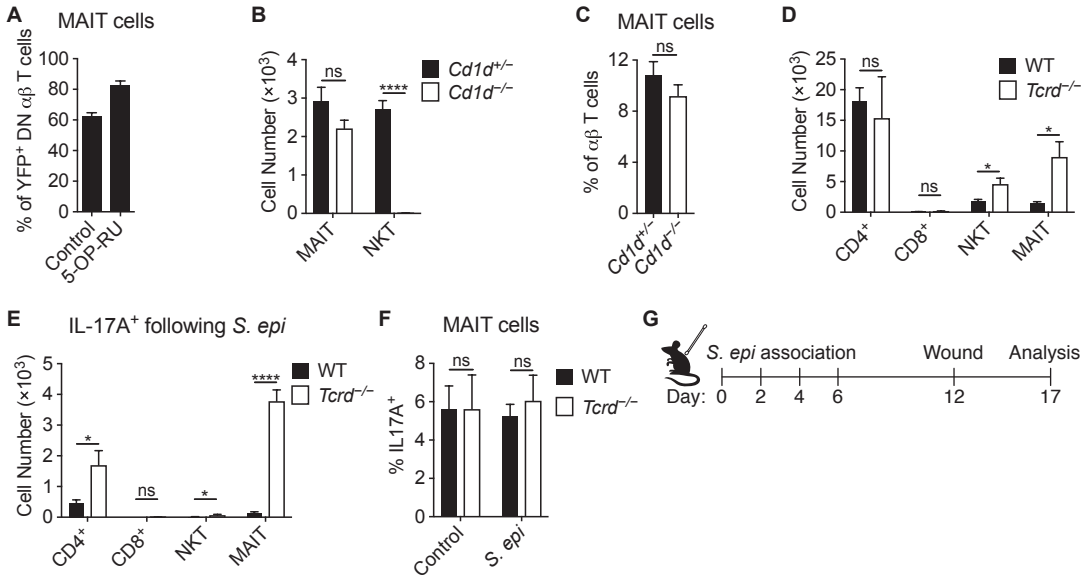

MAIT cells promote tissue repair. (**A**) Percentage of YFP$^+$ CD4$^-$ CD8$^-$ (double-negative; DN) TCRβ^+ $\alpha\beta$ T cells that are MAIT cells in the skin of *Il17a^{cre} R26-STOP-YFP* mice that received topical 5-OP-RU and untreated controls. (**B-C**) (**B**) Number and (**C**) frequency of cutaneous MAIT in *Cd1d$^{-/-}$* mice and *Cd1d$^{+/-}$* littermates. (**D**) Number of T cells in the skin of *Tcrd$^{-/-}$* and WT mice. (**E**) Number of IL-17A$^+$ T cells in the skin of *Tcrd$^{-/-}$* and WT mice following association with *S. epidermidis* LM061. (**F**) Percentage of MAIT cells that are IL-17A$^+$ in the skin of *Tcrd$^{-/-}$* and WT mice associated with *S. epidermidis* LM061 and unassociated controls. (**G**) Schematic depicting the wound healing experiment for Fig. 5E-F. Graphs indicate means ± SEM. Data represent at least two experiments with four or more mice per group. *p<0.05 and ****p<0.0001 as calculated by Student's *t*-test. "ns" denotes that comparison was not significant.

Table S1: List of flow cytometry antibodies for mouse (blue) and human (red).

Antibody	Clone	Fluorophore	Conc. (μg/mL)	Vendor	Catalog #
CD3	17A2	BV650	0.5	BioLegend	100229
CD4	RM4-5	BV605	0.5	BioLegend	100548
CD8b	H35-17.2	BV510	0.5	BD	740155
CD8b	eBioH35-17.2	FITC	1.25	eBioscience	11-0083-85
CD11b	M1/70	FITC	1.25	eBioscience	11-0112-82
CD11c	HL3	FITC	1.25	BD	557400
CD16/32	2.4G2	---	1.25	Bio-X-Cell	BE0307
CD24	M1/69	FITC	0.625	BioLegend	101806
CD25	PC61.5	APC	1	eBioscience	17-0251-82
CD44	IM7	AF700	1	eBioscience	56-0441-82
CD45	30-F11	APC-eF780	0.5	eBioscience	47-0451-82
CD45.1	A20	BV605	0.5	BioLegend	110738
CD45.2	104	APC-eF780	0.5	eBioscience	47-0454-82
CD45R	RA3-6B2	AF488	1.25	eBioscience	53-0452-82
CD49f	eBioGoH3	FITC	0.625	eBioscience	11-0495-82
CD90.2	30-H12	BV785	0.25	BioLegend	105331
CD218a	P3TUNYA	PE	2	eBioscience	12-5183-82
IFNγ	XMG1.2	eF450	2	eBioscience	48-7311-82
IL-17A	TC11-18H10.1	PE-Cy7	1	BioLegend	506922
Ki67	SolA15	FITC	2.5	eBioscience	11-5698-82
RORγt	B2D	APC	2	eBioscience	17-6981-82
TCRβ	H57-597	APC	0.5	eBioscience	17-5961-82
TCRβ	H57-597	PerCP-Cy5.5	0.5	eBioscience	45-5961-82
TCRγδ	GL3	BV650	0.5	BD	563993
TCRγδ	GL3	PE-CF594	0.25	BD	563532
CD3	OKT3	BV711	40	BioLegend	317328
CD45	HI30	BV650	0.1	BioLegend	304044
CD161	HP-3G10	PE-Cy7	0.1	BioLegend	339918

References *65-76*

65. K. Hirota *et al.*, Fate mapping of IL-17-producing T cells in inflammatory responses. *Nat Immunol* **12**, 255-263 (2011).
66. A. Awasthi *et al.*, Cutting edge: IL-23 receptor gfp reporter mice reveal distinct populations of IL-17-producing cells. *J Immunol* **182**, 5904-5908 (2009).
67. L. E. Jao, S. R. Wente, W. Chen, Efficient multiplex biallelic zebrafish genome editing using a CRISPR nuclease system. *Proc Natl Acad Sci U S A* **110**, 13904-13909 (2013).
68. S. Conlan *et al.*, Staphylococcus epidermidis pan-genome sequence analysis reveals diversity of skin commensal and hospital infection-associated isolates. *Genome Biol* **13**, R64 (2012).
69. I. R. Monk, I. M. Shah, M. Xu, M. W. Tan, T. J. Foster, Transforming the untransformable: application of direct transformation to manipulate genetically Staphylococcus aureus and Staphylococcus epidermidis. *MBio* **3**, (2012).
70. D. G. Gibson *et al.*, Enzymatic assembly of DNA molecules up to several hundred kilobases. *Nat Methods* **6**, 343-345 (2009).
71. D. E. Wright, A. J. Wagers, A. P. Gulati, F. L. Johnson, I. L. Weissman, Physiological migration of hematopoietic stem and progenitor cells. *Science* **294**, 1933-1936 (2001).
72. M. Lochner, H. Wagner, M. Classen, I. Forster, Generation of neutralizing mouse anti-mouse IL-18 antibodies for inhibition of inflammatory responses in vivo. *J Immunol Methods* **259**, 149-157 (2002).
73. J. A. Hall *et al.*, Essential role for retinoic acid in the promotion of CD4(+) T cell effector responses via retinoic acid receptor alpha. *Immunity* **34**, 435-447 (2011).
74. B. J. Callahan *et al.*, DADA2: High-resolution sample inference from Illumina amplicon data. *Nat Methods* **13**, 581-583 (2016).
75. M. Stoeckius *et al.*, Cell Hashing with barcoded antibodies enables multiplexing and doublet detection for single cell genomics. *Genome Biol* **19**, 224 (2018).
76. T. Stuart *et al.*, Comprehensive Integration of Single-Cell Data. *Cell* **177**, 1888-1902 e1821 (2019).